



Contents lists available at ScienceDirect

Journal of Nuclear Materials

journal homepage: www.elsevier.com/locate/jnucmat

High dose, up to 80 dpa, mechanical properties of Eurofer 97

Bob van der Schaaf^{a,*}, C. Petersen^b, Y. De Carlan^c, J.W. Rensman^a, E. Gaganidze^b, X. Averty^c^a NRG, Petten, 1755 ZG Petten, The Netherlands^b FZK, Karlsruhe, Germany^c CEA, Saclay, France

A B S T R A C T

In blankets of a fusion power plant 14 MeV neutrons produce displacement damage, dpa, and helium and hydrogen. Martensitic steels offer the advantages of low swelling and reduced helium embrittlement compared to austenitic steels. Reduced activation Eurofer 97 steel has been exposed to neutron displacement damage up to about 15 dpa in materials test reactors such as OSIRIS and HFR at temperatures in the range of RT to 600 °C, and up to 80 dpa in BOR-60 at temperatures in the range of 300–330 °C. The post-irradiation mechanical properties in the range of 300–330 °C show increases in yield stress, decrease in ductility and an increasing ductile to brittle transition temperature. The hardening rate is decreasing with increasing damage level, but it does not show saturation at doses examined. Analyzing the present results and reviewing properties of other steels with different compositions, including ODS steels, lead to the conclusion that improvement of the radiation resistance of steel will be based on nano-microstructural features.

© 2009 Published by Elsevier B.V.

1. Introduction

In fusion power plants blankets with lithium ceramics or liquid lithium lead will produce the tritium needed for the fusion reaction. The lifetime and reliability of the blankets require structural materials that are tough and strong during long periods of time to limit the remote exchanges of the blankets. Martensitic steels offer the advantages of low swelling and reduced helium embrittlement compared to austenitic steels. In addition the steel should show low activation to limit waste cost and the environmental impact [1]. Before much effort was devoted to chromium steel fast reactor cladding development [2], but the cladding temperature regime is way above that for fusion applications.

The implementing agreement of the IEA on fusion materials stimulated co-operation on development of low-activation martensitic steels in Japan, the US and the EU in the early nineties of the 20th century [3,4]. As long as there are no powerful 14 MeV sources such as IFMIF, the radiation resistance of these low activation steels, with compositions quite different from conventional steels, is tested with neutrons from fission reactions. The EU industrial scale reduced activation steel batch, Eurofer 97, has been exposed to neutron displacement damage up to about 15 dpa in materials test reactors such as OSIRIS and HFR at temperatures in the range of RT to 600 °C, and up to 80 dpa in the fast test reactor BOR-60 at temperatures in the range of 300–330 °C.

The present paper shows and interprets the major post-irradiation mechanical properties results such as yield stress, tensile ductility, and impact properties at radiation damage levels up to 80 dpa. The properties of other steels with different compositions, including ODS steels, are reviewed with the objective to show the potential roads to improvement of the steels radiation resistance.

2. Procedures

2.1. Materials and Specimens

The EU manufactured Eurofer 97 (9Cr-1W-0.2V-0.15Ta) on industrial scale; heat 83697 weighs more than 5000 kg. Heat 83697 was austenitized at temperatures between 960 and 1050 °C and tempered at a temperature around 760 °C during times dependent on the half product thickness. The Japanese reduced activation steel F82H mod. with 8.2Cr-2.2W-0.16V-0.02Ta was also included in the tests. In addition conventional 9Cr-1Mo (EM10) industrial steel is in the program:

Several laboratory melts such as OPTIFERIVc, manufactured by FZK with the composition 9Cr-1W-0.25V-0.07Ta, and JLF-1(basic composition 9Cr-2W-0.18V-0.08Ta) from the Japanese program with some minor composition varieties and heat treatment are also part of the program. Some laboratory scale heats have increased boron contents to boost the helium production. From the Eurofer 97 industrial scale cast Eurofer ODS steel was manufactured through atomization and ball-milling adding 0.5% Y₂O₃ followed by HIP. For comparison ODS-MA957 (14Cr-1Ti-0.3Mo-0.25 Y₂O₃) steel is tested in the program.

* Corresponding author. Tel.: +31 224564665; fax: +31 224568490.
E-mail address: vanderschaaf@nrg-nl.com (B. van der Schaaf).

The impact property tests utilized the KLST Charpy-V sub size specimens measuring $27 \times 4 \times 3$ mm. Tensile specimens had diameters in the range from 2 to 4 mm and gauge/diameter ratios were higher than five. Some of the tensile specimens were hour glass shaped to eventually allow fatigue testing.

2.2. Neutron irradiation

The materials test reactors HFR and OSIRIS used different types of rigs and irradiations capsules to irradiate the specimens at temperatures in the range of 45–600 °C with 15 °C absolute accuracy over the irradiation times lasting up to 3 years for 15 dpa. The cooling material of the rigs and irradiations capsules was sodium. Most specimens had thermocouples attached to check the temperature. The determination of radiation damage relied on gamma radiation of pure metal monitors extracted from the rigs in exact positions related to the specimens.

The neutron fluxes in the BOR-60 ARBOR irradiations amounted to about $1.8 \times 10^{19} \text{ n m}^{-2} \text{ s}^{-1}$. The temperatures of the specimens, submerged in sodium, remained under 340 °C for irradiations up to 80 dpa. In ARBOR-1 specimens were irradiated to about 40 dpa, some of these specimens were irradiated in ARBOR-2 to 80 dpa with negligible temperature and neutron flux gradients, and similar neutron spectrum.

2.3. Post-irradiation testing

Impact property test machines situated in hot-cells underwent calibration for maximum impact energies of 15 J from KLST specimens. The shielded tensile machines tested the small gauge tensile specimens after calibration adjusted for such small prey, smallest diameters 3 mm with gage length at least 18 mm. Post irradiation furnace temperature control was within the limits for the application, better than 5 °C deviation. Testing procedures were in line with the EU and ASTM standards.

3. Results

3.1. Analysis and determination of neutron doses

The neutron irradiations in the materials test reactors HFR, Petten [5,6], and OSIRIS, Saclay [7], and BOR-60 Dimitrovgrad [8], were carried out in capsules containing the specimens and neutron monitor sets. The neutron monitor sets consist of a group of pure materials pieces that undergo transmutation. The gamma radiation from the transmutation products allow the determination of the accumulated neutron fluence, and neutron spectrum experienced by the monitor set. From this neutron information the displacement damage, dpa, and fusion relevant transmutation products such as He and H in the irradiated structural materials are calculated using FISPACT. Then the measured values are extrapolated for each specimen; they reached to over 15 dpa maximally. The neutron damage generated in BOR-60 is calculated using the SPECTER code. In this case, the maximum damage value amounts to 80 dpa.

The temperatures in HFR, OSIRIS and Bor-60 capsules are measured [5–8] with several calibrated thermocouples. The measured values are interpolated for each individual specimen. The irradiation temperatures were in the range of 250–450 °C with 50 °C intervals. The deviations from the nominal test temperatures were 15 °C maximally.

3.2. Mechanical properties

Fig. 1 shows the increase of the yield stress as dependent on the displacement damage. The ferritic steels radiation hardening is

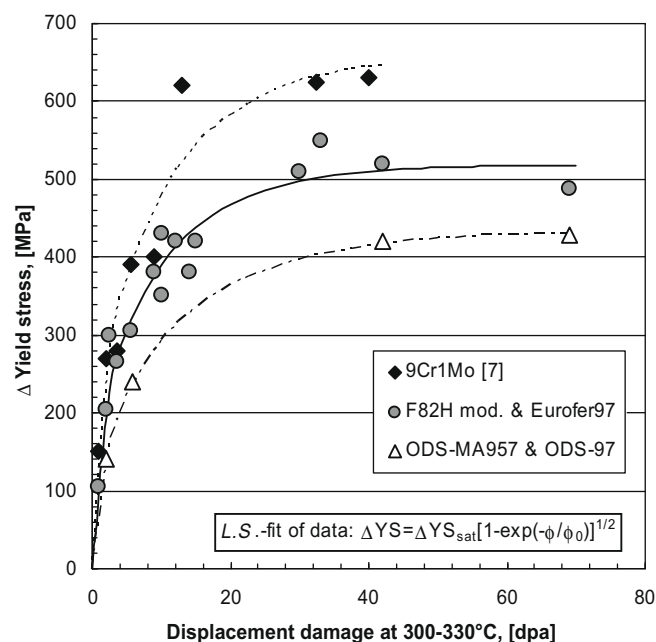


Fig. 1. The increase in yield stress of RAFM steels, conventional 9Cr steel and ODS steel MA957 as dependent on displacement damage at 300–330 °C.

quite steep below 10 dpa up to about 250 MPa (ODS steel), reduced activation steels up to 400 MPa, and up to 600 MPa for conventional chromium steels. Between 10 and 40 dpa the increase is about 150 MPa for reduced activation steel. Thus in the first 10 dpa the hardening rate is between 25 and 60 MPa.dpa⁻¹, whereas over 10 dpa the hardening rate is between 5 MPa.dpa⁻¹, a rate decrease of an order of magnitude. The experiments to show hardening saturation to be reached at 80 dpa have not yet been conducted, but will be soon.

The total ductility of conventional chromium steels continuously decreases to values below 1% at 43 dpa, whereas RAFM and ODS-MA957 steel MA show total elongations over 5% up to 43 dpa. The uniform elongation of conventional and RAFM steel is below 1% at radiation levels over 10 dpa; ODS-MA957 shows 1% uniform elongation over 10 dpa.

Fig. 2 shows the impact energies measured in different steels in reference and irradiated conditions up to 80 dpa. The radiation damage increases the DBTT of the different steels by 150–240 °C. The upper shelf energy, USE, of the RAFM steels is nearly halved; of the conventional 9Cr steels the USE is reduced to 20% of its reference level.

Fig. 3 shows the increase in DBTT plotted versus the displacement damage resulting in three curves that show similarity with the tensile hardening curves shown in Fig. 1. The 9Cr1Mo steels show the largest hardening and ODS steel is the least affected by radiation damage. The RAFM Eurofer steels take a position in between, but they do not show DBTT saturation.

It must be stressed that the irradiation temperatures are between 300 °C and about 330 °C. At this temperature the hardening is at its highest level. Over 330 °C the radiation hardening rapidly decreases to zero around 425 °C.

3.3. Fractography

Fig. 4 shows the SEM pictures of tensile fractures. They are typical for Eurofer 97 specimens tested at 300 °C in air with a strain rate of $1 \times 10^{-3} \text{ s}^{-1}$ after irradiation in BOR 60 at 300 °C and 15 dpa. The fracture appearance is still very ductile with the dimple structure containing hard inclusions.

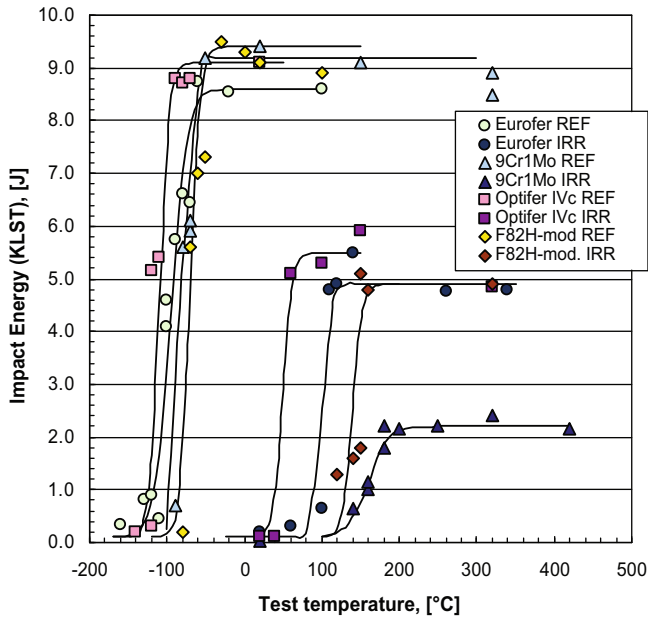


Fig. 2. The impact energy of RAFM steels, Eurofer, OPTIFER and F82H mod., and conventional 9Cr steel in neutron irradiated (at 300–330 °C) and reference condition versus test temperature.

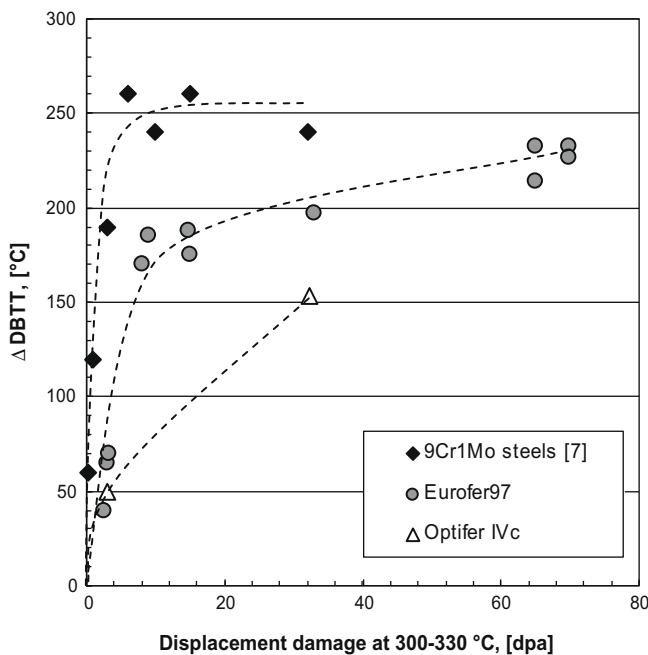


Fig. 3. Increase in DBTT of RAFM, conventional and ODS steel versus the displacement damage generated at 300 °C.

They show typical cup and cone fracture with a 65% reduction of area, underpinning the ductility data retrieved from post-irradiation tensile curves, though uniform elongation amounts to less than 1%.

Fig. 5 shows the fracture surfaces of impact tested KLST specimens at 30 dpa. The lower shelf specimens show no deformation at all, whereas specimens fractured in the upper shelf show deformation. The upper shelf results show somewhat more deformation for the higher austenitization temperature. These results are typical for the high dose irradiation effects on impact fracture appearance.

4. Discussion

4.1. Strength and ductility

Fig. 1 shows that the increase in yield stress reaches saturation somewhere near 40 dpa. The data points at 64 and 69 dpa are at levels similar to those observed at 30 and 40 dpa and at least in the scatter band for the data. Yamamoto et al. recently analyzed the effects of irradiation on yield stress in 8Cr tempered steels [9]. Whapham and Makin earlier explained the effect of displacement damage on the increase in yield stress [10]. Whapham and Makin argue that in the early stages the radiation particles, in our case neutrons, produce lattice damage creating obstacles for dislocation movement. At first the obstacle production is linear with the radiation damage, and hence the yield stress increases with the square root. At higher damage levels the existing obstacles capture the newly formed ones leading to saturation of the obstacle density, and thus the yield stress. They derive the equation:

$$\Delta YS = \Delta YS_{\text{sat}} [1 - \exp(-\phi/\phi_0)]^{1/2} \quad (1)$$

where,

ΔYS = the increase in yield stress from radiation damage

ΔYS_{sat} = the saturated yield stress from radiation hardening

ϕ = radiation dose

ϕ_0 = scaling factor depending on radiation conditions such as temperature

Dimelfi [11] showed for other ferritic reactor pressure vessel steels that the Whapham and Makin model is valid, but for a narrower damage window than the present experimental conditions. The present experimental evidence up to 70 dpa supports the saturation model proposed by Whapham and Makin for the RAFM and conventional steels investigated in the HFR, OSIRIS, and the ARBOR-2 experiment in BOR-60.

The total elongations of RAFM steels neutron irradiated up to 70 dpa measure at least 10% and reductions of area are in excess of 50%. The deformability of the material is thus considerable, though it is not uniformly spread over the specimen gauges, because the uniform elongation derived from the tensile curve is under 1%, down to a few tenths of a percent. After reaching its peak stress the deformation continues to spread over the specimen. This observation suggests a mechanism whereby initiation of dislocation movement is inhomogeneous distributed, followed by a phase in the test where unpinning of dislocations is more homogeneous. The precise development must be derived from additional microscopy.

The role of helium cannot be studied adequately with fission reactors, but it might have an appreciable effect on the deformation mechanism [12]. In the end fusion environment simulators such as IFMIF, must provide the experimental evidence for the interaction of displacement damage and transmutation produced helium.

The ODS steel shows total and uniform elongations of 4.5% and 1.2%, respectively, indicating a different dislocation movement initiation and propagation. In the ODS steel case besides the displacement damage to the lattice, the dispersions have a strong effect on ductility.

4.2. Impact properties

Fig. 3 shows that the increase in DBTT has not saturated. The ΔDBTT for values near 70 dpa are significantly, about 10–20 °C higher than the DBTT observed at about 35 dpa. The USE though does not differ significantly for the irradiation damage interval

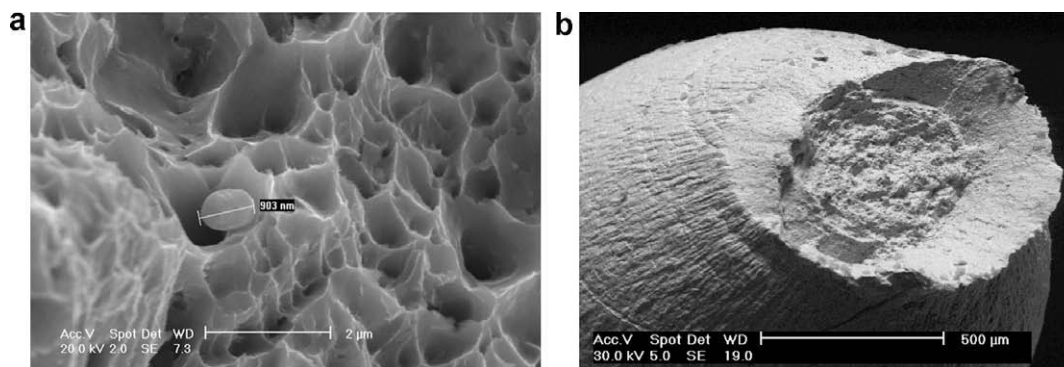


Fig. 4. (a) Detail of tensile fracture at 300 irradiated to 15 dpa in BOR-60, (b) Necking of tensile specimen at 300 irradiated to 15 dpa in BOR-60.

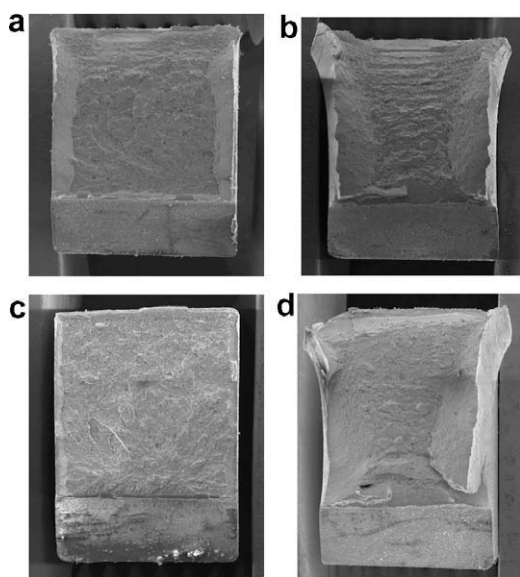


Fig. 5. (a) Fracture of lower shelf impact of Eurofer (anneal 980 °C) tested after 30 dpa, (b) Fracture of upper shelf impact of Eurofer (anneal 980 °C) tested after 30 dpa, (c) Fracture of lower shelf impact of Eurofer-2 (anneal 1040 °C) tested after 30 dpa, (d) Fracture of upper shelf impact of Eurofer-2 (anneal 1040 °C) tested after 30 dpa.

from 15 to 70 dpa. These observations lead to the conclusion that the RAFM material still can absorb considerable energy. The onset of energy absorption though starts at an increasingly higher temperature. In contrast with the tensile hardening saturated over 50 dpa, the ductile impact response is at a still higher temperature.

Fig. 6 shows the DBTT increase and USE reduction for the different materials irradiated to 32 dpa at about 332 °C. There seems to be a weak correlation of the DBTT shift and the USE reduction. The outlier is an ODS steel with a non-optimized production path. It has already a very low USE in the reference condition and the radiation hardly affects it. A correlation between USE and DBTT shift is not very significant.

Comparing Δ DBTT values observed for different irradiated RAFM steels at different temperatures [3] it becomes evident that there is a strong separation in deformation and irradiation regime at about 350 °C. Below 350 °C high Δ DBTT values are observed, above 350 °C Δ DBTT values are negligible. Microscopic studies show a dramatic reduction in the damage density, explaining the experimental observation, [13].

4.3. Effects of steel composition and microstructure

The control of the impurities in the steels dramatically improves the mechanical properties and especially the toughness

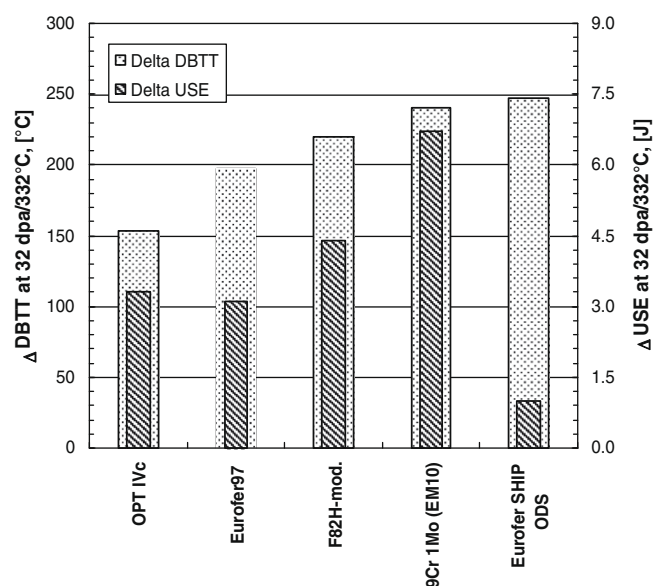


Fig. 6. Increase in DBTT and Upper Shelf Energy, USE, versus the DBTT measured for different steels at 300 °C.

[14]. A homogeneous microstructure without delta ferrite, large inclusions or carbides and without intermetallics is very favorable for the behavior of the material. However, the influence of Cr, W, Mo, Ta, V is not so clear. Further it is difficult to quantify the effects for each of these major elements from the integrated results.

The behavior of ferritic/martensitic materials after neutron irradiation at temperatures near 325 °C depends strongly on their fabrication process and microstructure. The ODS MA957 considered in this study has a microstructure which in some point reminds a martensitic steels with very fine laths. Contrary to martensitic materials, in fine grain ODS, the “laths” are much longer and with almost the same crystallographic orientation, but the analogy to a martensitic microstructure is clear. It appears that this type of microstructure, with very high densities of boundaries or interfaces resists neutron exposure the best. Without considering the helium embrittlement, the presence in the macrostructure of nano-phases like nano-oxides (present in the MA957 material) or nano-carbonitrides (present in the Eurofer but not in the 9Cr 1Mo steel) seems to improve also the behavior of the material. The 9Cr1Mo steels, which is the softest material with a very low DBTT before irradiation exhibit a high hardening under irradiation and present the most important shift of the DBTT among the materials after irradiation.

4.4. Extrapolation of properties and potential improvements

Despite the remarkable results obtained within the European framework and especially the improvement of the DBTT of martensitic steels before and after irradiation, the challenge to obtain a martensitic steel as structural material for fusion power plants remains open. After irradiation at low temperature (325 °C or below), a saturation of the hardening and of the increase of the DBTT was expected. The latest results show that this is not the case and no martensitic/ferritic materials seems to be available for such low temperatures. A close cooperation between designers of fusion power plants and material scientists has to take that major point into account. The crucial issues that have to be resolved are probably the displacement hardening after irradiation, and the helium embrittlement. As mentioned above, at 400 °C the neutron irradiation of ferritic/martensitic steels is much less severe for the material. The operating window of the martensitic steels has to be shifted toward higher temperatures, maybe up to 650 °C with a lower limit near to 400 °C. The design of new martensitic materials for fusion application has then to be rethought in the direction of nano-microstructural features (Section 4.3. Different tentative results have already been published [5,15]. The use of the new thermo-kinetic calculation models (MatCalc or Dictra for example) will guide the development further.

5. Conclusion

1. Tensile hardening shows saturation at 70 dpa and 330 °C. This is not the case for impact properties. The DBTT at 70 dpa and 330 °C still increases by about 25 °C. The Whapham and Makin saturation radiation hardening model works well for tensile properties. It does not work perfectly well for impact fracture of Eurofer steels, but the impact deformation rate is many orders of magnitude higher than that under normal tensile conditions.
2. Microstructures with high interface densities (grain boundaries or laths) of low activation steels seem beneficial for neutron radiation resistance in comparison with conventional steels coarser micro-structural features, irradiated to radiation damage levels similar to 70 dpa.
3. The paths to more radiation resistant ferritic/martensitic steels will be guided by thermo-kinetic codes to limit the necessary experimental verification to the essentials. The direction of development is nano-microstructural features that promise to improve the radiation resistance in steels.

Acknowledgements

This work, supported by the European Communities under the contracts of Association between EURATOM/FOM-NRG, FZK and CEA, was carried out within the framework of the European Fusion Development Agreement. The views and opinions expressed herein do not necessarily reflect those of the European Commission.

References

- [1] G.J. Butterworth, L. Giancarli, J. Nucl. Mater. 155–157 (1988) 575.
- [2] J.M. Dupouy, French Program on LMFBR Cladding Materials Development, in: Proceedings of International Conference: Radiation effects in Breeder Reactor Structural Materials, Metallurgical Society of AIME, New York, 1977, pp. 1.
- [3] Proceedings of the IEA Workshop on Ferritic/Martensitic Steels, JAERI, Tokyo, Japan, 26–28 October 1992.
- [4] A. Hishinuma, A. Kohyama, R.L. Klueh, D.S. Gelles, W. Dietz, K. Ehrlich, J. Nucl. Mater. 258–263 (1998) 193.
- [5] J.W. Rensman, Report on 300 °C and 60 °C irradiated RAFM steels, NRG report 68497, Petten, 2005.
- [6] E. Gaganidze, H.-C. Schneider, B. Dafferner, J. Aktaa, J. Nucl. Mater. 355 (2006) 83.
- [7] A. Alamo, J.L. Bertin, V.K. Shamardin, P. Wident, J. Nucl. Mater. 367–370 (2007) 54.
- [8] C. Petersen, J. Aktaa, E. Diegele, E. Gaganidze, R. Laesser, E. Lucon, E. Materna-Morris, A. Moeslang, A. Povstnyanko, V. Prokhorov, J.W. Rensman, B. van der Schaaf, IAEA- CN-149 Fusion21 proceedings, Wien, ISBN 92-0-100907-0/ISSN 0074-1884.
- [9] T. Yamamoto, G.R. Odette, H. Kishimoto, J.-W. Rensman, P. Miao, J. Nucl. Mater. 356 (2006) 27.
- [10] A.D. Whapham, M.J. Makin, Phil. Mag. 5 (1960) 237.
- [11] R.J. Dimelfi, D.E. Alexander, L.E. Rehn, Report ANL/RE/CP-98154, 1999.
- [12] J. Henry, L. Vincent, X. Averty, B. Marini, P. Jung, J. Nucl. Mater. 367–370 (2007) 411.
- [13] R.L. Klueh, D.L. Harries, High Chromium Ferritic And Martensitic Steels For Nuclear Applications, ASTM Monograph 3, West Conshohoken, ASTM, PA, USA, p. 139.
- [14] Y. De Carlan, M. Muruganath, T. Sourmail, H.K.D.H. Bhadeshia, J. Nucl. Mater. 329–333 (2004) 238.
- [15] R.L. Klueh, N. Hashimoto, P.J. Maziasz, Development of new nano-particle-strengthened martensitic steels, Scripta Mater. 53 (2005) 275.